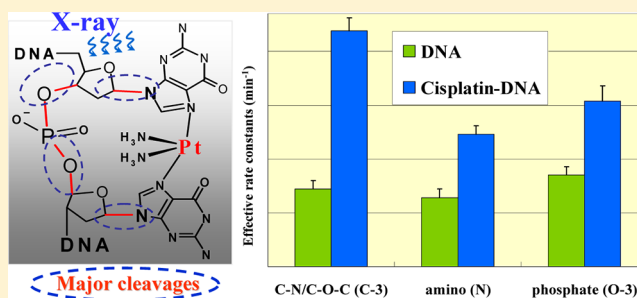


Cleavage Enhancement of Specific Chemical Bonds in DNA by Cisplatin Radiosensitization

Fangxing Xiao, Xinglan Luo, Xianzhi Fu, and Yi Zheng*

Fujian Provincial Key Laboratory of Photocatalysis, State Key Laboratory Breeding Base, College of Chemistry and Chemical Engineering, Fuzhou University, Fuzhou 350002, People's Republic of China

ABSTRACT: X-ray photoelectron spectroscopy (XPS) is harnessed as an in situ efficient characterization technique for monitoring chemical bond transformation in DNA and cisplatin–DNA complexes under synergic X-ray irradiation. By analyzing the variation of relative peak area of core elements of DNA as a function of irradiation time, we find that the most vulnerable scission sites in DNA are those containing phosphate and glycosidic bonds. Compared to DNA, the effective rate constants of the corresponding phosphodiester and glycosidic bond cleavages for cisplatin–DNA complexes are 1.8 and 1.9 folds larger. These damages and their enhancements are similar to those induced by low energy electrons (LEE). Consistently, the magnitude of the secondary electron distribution produced by the X-rays on the cisplatin–DNA complexes is considerably increased compared to that of pristine DNA. The data suggest that DNA radiosensitization by cisplatin results not only from the sensitization of DNA to the action of LEE, but also from an increase the production of LEE at the site of binding of the cisplatin. The results provide new insights into the mechanisms of cisplatin-induced sensitization of DNA under X-ray irradiation, which could be helpful in the design of new cisplatin-based antitumor drugs.



1. INTRODUCTION

In the history of the exploration of anticancer drugs, one significant hallmark is the discovery of cisplatin [Pt-(NH₃)₂Cl₂],^{1–4} which to date remains as one of the most frequently used chemotherapeutic agents for treatment of various cancers.^{5–8} Many investigations regarding the cytotoxic properties of cisplatin in chemotherapy have revealed that cisplatin exhibits intrinsic bonding to DNA at the N7 sites of guanine and adenine, thereby generating intrastrand and interstrand cross-linking, and monofunctionally bound DNA adducts.⁹ In malignant cells, these transformations could be mutagenic or lethal.¹⁰ In this regard, the interaction between cisplatin and DNA constitutes the basis of its chemotherapeutic mechanism and plays the key role in clinical administration.

The combination of many therapies, including radiotherapy, surgery, and chemotherapy, has become the standard modality in the clinic for many decades in order to achieve better cancer treatment. A frequent strategy relies on the combination of chemotherapy and radiotherapy. This modality, named chemoradiation therapy (CRT), is a standard treatment option for many types of solid tumors. Recently, utilizing cisplatin in the concomitant CRT of tumor cells has attracted considerable interests.^{5,6} Under certain conditions in concomitant CRT, cisplatin can become a radiosensitizer in addition to being a chemotherapeutic agent. In this case, the damage in tumor cells becomes larger than with chemotherapy and radiotherapy delivered separately. However, the basis of synergic interaction between the radiation and the Pt-drug in vivo remains unclear.

Essentially two mechanisms related to the binding of cisplatin to DNA have been proposed.¹¹ One interpretation of the synergistic effect is due to the inhibition of repair of radiation-induced damage to DNA.¹² Another possibility is that the immediate species created by the primary radiation in cells cause additional damage when cisplatin is covalently bonded to DNA. So far, the latter mechanism for increased DNA radiosensitivity from the binding of Pt-based antitumor drugs is still a controversial debate, because fundamental information on the detailed chemical bond transformation of DNA during high energy irradiation is not yet available. Kobayashi et al. reported that DNA bound to platinum containing molecules was inclined to suffer from substantial strand-break enhancement under concomitant X-ray irradiation.¹³ Zheng et al.¹⁴ reported that bombarding solid films of DNA–cisplatin complex with different electron energies (1, 10, 100, and 60000 eV) significantly promotes strand breaks of DNA by factors varying from 1.3 to 4.4. These authors proposed that configuration distortion of DNA and the increase in cross section for the interaction of low energy secondary electrons (SE), induced by cisplatin, contributed to the enhancement of cell killing with the radiation.¹⁵ Luo et al.¹⁶ presented a dissociative electron-transfer mechanism concerning the action of cisplatin, which implied that the influence of cisplatin exerted on DNA in the concomitant irradiation could be elucidated by

Received: January 25, 2013

Revised: March 26, 2013

Published: April 3, 2013

studying the specific interaction between cisplatin and DNA. The purpose of the present study is to compare the high energy radiation results with those obtained with LEE¹⁴ to examine if the superadditive effect observed in tumor regression may be related, at least partly, to the enhancement of LEE production.

The analysis of the most important target in CRT (i.e., DNA) after irradiation have been carried out with a collection of techniques, such as agarose gel electrophoresis,^{17,18} high performance liquid chromatography (HPLC),^{19,20} and high performance liquid chromatography, combined with various sophisticated mass spectroscopy analysis (e.g., HPLC-MS).^{21–23} For example, supercoiled reduction, single-strand break (SSB) and double-strand break (DSB), as well as cross-link of DNA after irradiation, could be characterized by agarose gel electrophoresis.²⁴ Nevertheless, these conventional techniques are inevitably time-consuming. X-ray photoelectron spectroscopy (XPS), on the contrary, is a straightforward and powerful quantitative spectroscopic technique, which can quickly collect profuse information on detailed elemental composition, empirical formula, chemical state, and electronic state of the elements within a sample by measuring the kinetic energy and number of electrons escaping from the top 1 to 10 nm of the surface of the material being analyzed. More significantly, XPS can also probe modifications in the bonding energy within functional groups and, thus, chemical bond transformations, by appropriate Gaussian fitting.²⁵

In this study, XPS is utilized simultaneously as a radiation source of soft X-ray and an *in situ* characterization tool to trace the chemical bond modifications in DNA and DNA–cisplatin complexes. By analyzing the alternation in the intensity of Gaussian-fitted peak areas correlated to varied chemical bonds of DNA, the radiosensitization of cisplatin binding to DNA is monitored *in situ* via XPS. In previous experiments, Ptasinska et al. monitored thymus DNA damage under X-ray by XPS.²⁶ We apply a similar method with improved resolution to study specific chemical bonds cleavages in DNA by X-ray photons with and without the chemotherapeutic agent cisplatin. The comparison of XPS core-level spectra for the elements O, P, N, and C during the course of irradiation show that the most vulnerable scission sites in DNA involve phosphodiester and glycosidic bonds, which correspond to typical low-energy electron (LEE)-induced DNA damages. Consistently, the production of SE for cisplatin–DNA complexes by X-ray radiation greatly increases compared to DNA. The result suggests that the binding of cisplatin to DNA markedly contributes to enhance chemical bond transformation induced by 1.5 keV X-ray irradiation. Considering the results of previous experiments,^{14,15} thus, the mechanism of Pt-based chemoradiation therapy, could involve both a rise in production of LEE and the increased sensitivity of DNA mostly via LEE interaction in the initial physicochemical stage of the radiation.

2. EXPERIMENTAL SECTION

2.1. Preparation of DNA. pGEM-3 Zf (–) plasmid DNA (3197 bp, Progmega) was extracted from *Escherichia coli* DH5 α and purified with the QIAfilter plasmid Giga kit (QIAGEN). Agarose gel electrophoresis analysis showed that the supercoiled, concatemeric and nicked circular forms account for 91, 0.03, and 8.97%, respectively, in the purified plasmid DNA. The plasmid DNA concentration was obtained by measuring its absorption at 260 nm, which 1 O.D. corresponds to DNA of 50 ng/ μ L. The ratio of UV absorbance at 260 (A260) to 280 nm is measured to be 1.91.

Calf thymus DNA with molecular weight of $10\text{--}15 \times 10^6$ Da was purchased from Sigma and used without further purification. Thymus DNA is prepared from male and female calf thymus tissue and contains predominantly double-stranded DNA. DNA of calf thymus is 41.9 mol % G-C and 58.1 mol % A-T. From the molecular weight, we can estimate the helix of thymus DNA is of 17–25 kbp, which is about 5–7 times longer than plasmid DNA. The ratio of A260/A280 for thymus DNA of 1.91 was the same as that obtained for plasmid DNA, which indicates both double-stranded DNA contain relatively the same amount of impurities.^{27–29} In the following content, we generally refer DNA to the extracted plasmid while specifying thymus in its utilized experiment of Pt 4f spectra.

2.2. Preparation Films of Plasmid DNA and Cisplatin–DNA Complex. A total of 10 μ L of 21.4 μ g plasmid DNA was deposited on the tantalum film (Alfa Aesar, 99.95%, ultrasonically washed by ethanol and ddH₂O for three times before deposition) and dried in a glovebox with a nitrogen atmosphere at room temperature, thus, forming pure plasmid DNA film with thickness of about 1 μ m.¹⁴ *cis*-Diammineplatinum(II) dichloride (cisplatin) was obtained from Sigma Aldrich and used without any further purification. A 0.5 mg aliquot of cisplatin was dissolved in 500 μ L of dd H₂O at 55 °C for 30 min in PCR (GeneAmp PCR System 9700), producing cisplatin aqueous solution with a concentration of 1 μ g μ L^{–1}. The solution was diluted to 10 ng μ L^{–1}, mixed with DNA at molar ratio (R) of 8:1 and heated at 37 °C for 4 h to obtain the cisplatin–DNA complex. The cisplatin–DNA solution was used to prepare the condensed film with the same thickness of about 1 μ m, assuming the contribution of adding cisplatin to the film thickness is negligible. The cisplatin–thymus DNA complexes were similarly prepared. The specific manipulation process was the same as that of pure DNA, as mentioned above. Thereafter, films of DNA, cisplatin–DNA, and cisplatin–thymus complexes deposited on the tantalum were immediately transferred to the XPS chamber for vacuum-pumping overnight.

2.3. X-ray Irradiation and XPS Measurement. XPS measurements were conducted using a commercial XPS system (Thermo Scientific ESCALAB 250) equipped with a dual anode X-ray source, a concentric hemispherical electron energy analyzer, and a magnetic electron lens. The apparatus was operated with a monochromatized Al K α beam as the excitation source ($h\nu = 1486.6 \pm 0.45$ eV, work function: 4.38 eV) having an emission current of 6 mA at a base pressure of 3.8×10^{-10} mbar. Pure DNA and cisplatin–DNA complexes were continuously irradiated by the X-ray beam for 3 h. The XPS spot size and analyzer field of view were below 1 mm². At each interval time of 15 min, the survey and high-resolution spectra of C 1s, O 1s, N 1s, P 2p from DNA as well as Pt 4f from cisplatin and cisplatin–DNA were recorded. Simultaneously, the neutralizing electron gun was turned on to eliminate charging of the samples during X-ray irradiation. To ensure that the electron beam produced negligible DNA damage due to electron irradiation, the energy of the electrons and the current were kept as low as possible, by placing a bias voltage of 2 eV between the target and the filament of the flood gun and by keeping the current passing through the target below 200 ± 50 pA. Judging from the stability in energy of the XPS spectra, which within 0.2 eV, barely shifts, for the identical sample during the X-ray irradiation, this current was sufficient to avoid significant charging of the targets. XPS spectra were recorded for survey scans and high-resolution scans, corresponding to

pass energy of 100 eV, 50 eV with an energy step size of 1 eV, and 0.05 eV, respectively. The survey scans with binding energy (BE) ranging from 0 to 1200 eV were recorded for compositional analysis. All the core-level spectra were calibrated by shifting the C 1s binding energy line to 285.0 eV, which corresponds to standard hydrocarbon energy of C–H and C–C bonds.

2.4. XPS Peak Fitting. The high-resolution spectra of the elements were fitted using commercial XPS analysis software (Advantage 4.37). The peaks of individual core-level spectra were convoluted with Lorentzian and Guassian line shapes in the fitting procedure. The background was modeled with a Shirley function. The peak area and ratios for the various elements were corrected by experimentally determined instrumental sensitivity factors within an accuracy of $\pm 5\%$.

2.5. Measurement of Secondary Electron Distribution. Cisplatin–plasmid–DNA complexes with *R* of 8:1 were prepared by using the procedure described in section 2.2. Films of DNA, cisplatin, and cisplatin–DNA (*R* = 8) of 300 nm thickness were transferred to the XPS chamber. The SE emission measurements were performed in the LEE mode with the pass energy of 0.8 eV and energy step of 0.05 eV without the neutralizing gun.

3. RESULTS AND DISCUSSION

3.1. Bond Transformation in Cisplatin–DNA Complexes under X-ray Irradiation. The high-resolution XPS spectra of C 1s, O 1s, N 1s, and P 2p for the cisplatin–DNA complexes before and after irradiation of 1.5 keV X-ray for 3 h are exhibited in Figure 1. Owing to the effects of bonding

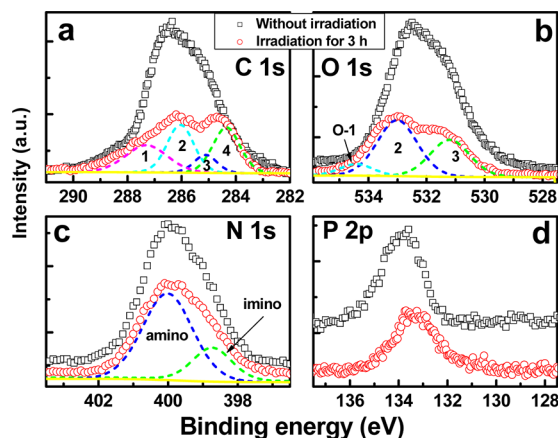


Figure 1. High-resolution XPS spectra of (a) C 1s, (b) O 1s, (c) N 1s, and (d) P 2p for cisplatin–DNA complex (*R* = 8) before irradiation (□) and irradiated for 3 h (○). The peaks of postirradiation are deconvoluted into specific components of each element in DNA (dashed line) including (a) urea (C-1), amide (C-2), C–N/C–O–C/C–OH/N=C–C (C-3), and hydrocarbon (C-4); (b) C–OH (O-1), C=O/N=O (O-2), and phosphate (O-3); (c) amino and imino.

electrons on the binding energy (BE) of core electrons, an XPS spectrum can be deconvoluted into several subpeaks corresponding to specific chemical bonds. Accordingly, the chemical composition can be characterized by XPS from the BE and by integration of the deconvoluted subpeak in the high-resolution spectrum. In this manner, the relative amount of each element can be estimated within the probing depth. The XPS characterization of these bonds for DNA²⁶ and cisplatin–DNA complexes have been reported previously.³⁰ The same

assignments relating to the four principal elements apply to the present study. For clarity, the deconvoluted peaks are only noted in the spectra of postirradiation (Figure 1).

The BE of specific chemical bonds, which were deconvoluted from the main peaks, did not exhibit shifts less than about 0.2 eV during bond breaking and desorption. On the other hand, the peak intensities decreased appreciably for the C 1s and O 1s spectral lines during irradiation, while the BE of each element remained the same. This behavior reflects a significant modification of the relative mass content of carbon and oxygen with X-ray exposure. We must therefore postulate that some evaporable molecules or ions (e.g., CN, OCN, CH₃[−], O[−], OH[−] and CN[−]) are formed as the result of bond scission and desorb from the sample surface. Several small neutral and anionic fragments desorbing from DNA films via the formation of transient negative ions have been detected by electron stimulated desorption (ESD).^{31,32} The most abundant species were CN, OCN, CH₃COOH, H[−], CH₂[−], CH₃[−], O[−], OH[−], and CN[−], which may provide some explanation for the decreasing of peak intensity in the present study.

Figure 2 shows the peak area of assigned chemical bonds as a function of irradiation time. Among the carbon species displayed in Figure 2a, hydrocarbon (C–C/C–H, C-4) and amide carbon (N–C=O, C-2) do not exhibit decreasing trend in area, but rather increase to about 17 and 22% at 15 min, which is retained during further irradiation. On the contrary, C–N/C–O–C/C–OH/O–C–N (C-3) and N–C(=O)–N (C-1) species demonstrate a decreasing amplitude to about 65.36 and 14.90% at 180 min. The strongest decay in peak area of C-3 indicates that X-ray irradiation preferentially leads to the related bond scission compared with other carbon species, that is, C–N/C–O–C/C–OH/O–C–N may be the most vulnerable sites in the cisplatin–DNA complex, which correlate to the chemical bonds within the base and sugar moieties. The most intense neutral fragments desorbing from oligonucleotides bombarded with 1–30 eV electrons that could be detected by the mass spectrometry are CN, OCN, and H₂NCN.³² Our result of dramatic decrease of C-3 bonds has good agreement with the most likely desorption of CN and OCN induced by LEE. The systematic investigations of ionization radiation of DNA and LEE-induced DNA damage support the occurrence of similar bond cleavages.^{33,34} The glycosidic bond (C–N) cleavage of DNA leading to the release of bases is one of the most intense damage induced by LEE bombardment.³⁴ The rise in signal of the C-2 and C-4 species may be caused by the synergistic contribution of C-3 bond scission leading to the increase of hydrocarbon (C–C/C–H) and amide carbon (N–C=O) species.

In the case of nitrogen species (Figure 2b), amino and imino sites display different trend. The amino peak monotonically decreases at early irradiation time and gradually maintains intensity of 70% with irradiation time processing. The imino peak presents no substantial variation during the first 90 min but abruptly decreases by about 10% and keeps steady for the rest of irradiation time. This result indicates that amino sites (NH–C, NH₂, or N–C) are more likely to undergo bonds scission than imino sites (–N=C) under X-ray exposure, which is in good agreement with the breakage of C-3 bonds. In other words, the two consistent most decreasing species observed from C and N elements could be eluded from identical chemical bond involving N–C. The decreased peak intensity may be ascribed to the dehydrogenation of amino and scission of N-glycosidic bond.

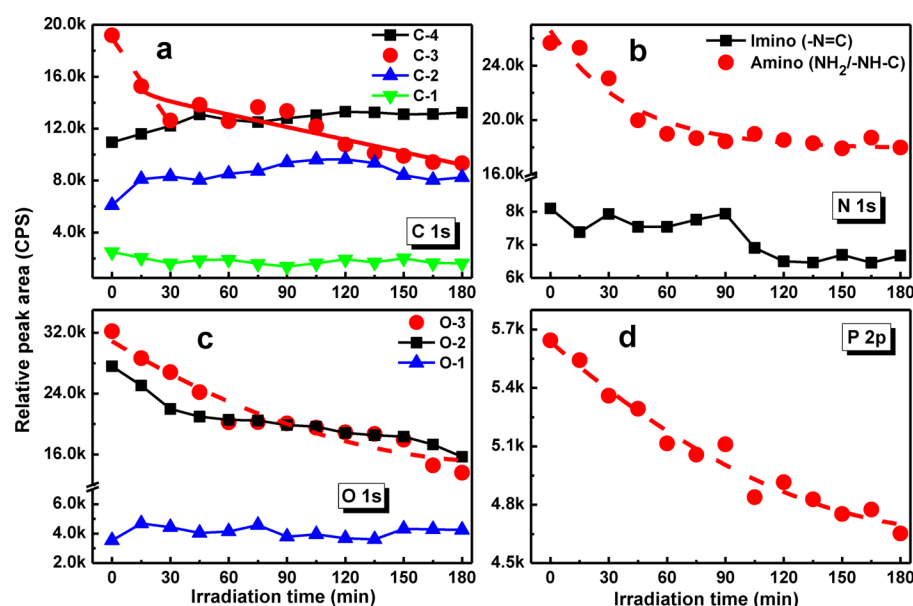


Figure 2. Peak area of deconvoluted subpeaks in the high-resolution XPS spectra of compositional elements (a) C 1s, (b) N 1s, (c) O 1s, and (d) P 2p as a function of X-ray irradiation time for cisplatin–DNA ($R = 8$).

Table 1. Comparison of Effective Bond Breakage Rate Constants (min^{-1}) for DNA and Cisplatin–DNA Complexes Induced by X-ray Irradiation^a

target	C-3 (C–N/C–O–C)	N (amino)	O-3 (phosphate)	P (phosphate)
DNA	72 ± 16	64 ± 8	85 ± 15	9.4 ± 3.7
cisplatin–DNA	219 ± 24	123 ± 16	154 ± 28	8.9 ± 1.1

^aThe error is the standard deviation in the corresponding first-order or pseudo-first-order fit to the data of Figure 2.

Figure 2c displays a variety of oxygen species. Oxygen in the phosphate group (O-3) and carbonyl/amide group (O-2) show similar decrease trend to 56.85 and 39.36%, respectively. On the contrary, O-1 (C–OH) remains relatively stable during the irradiation. O-3 characterizes the DNA backbone. The nearly half decrease of O-3 indicates that cisplatin radiosensitization could significantly induce DNA strand breaks. Consistently, P2p, which could only come from phosphate in DNA, shows a similarly decreasing trend as that of O-3 (Figure 2d).

The XPS analysis shows that the most probable chemical bond transformations of cisplatin–DNA complexes by X-ray irradiation are C-3, amino-N, O-3, and phosphate. Interestingly, the kinetics of these four chemical bonds show similar first order or pseudofirst order (dashed lines in Figure 2). Applied the first order or pseudofirst order rate equation, the effective rate constant of the four chemical bonds for cisplatin–DNA are listed in Table 1. It has been well-established that cisplatin efficiently targets DNA and binds preferentially to guanine at N7 site to generate interstrand and intrastrand cross-link adducts.^{10,35} The binding modifies DNA duplex to contain an unusual juxtaposition of A-like and B-like helical segments.³⁶ The resulting bending structure of DNA could from one aspect explain the enhanced radiosensitization induced by cisplatin.

3.2. Comparison of Cisplatin–DNA with DNA. The comparison of N 1s and O 1s spectra for DNA and cisplatin–DNA complexes before and after irradiation for 3 h are displayed in Figure 3. It has been shown that the introduction of cisplatin generally induces substantial positive BE shifts of DNA elements compared to that of pure DNA.³⁰ Consistently, before irradiation for N 1s, the amino and imino species of cisplatin–DNA complexes shift to higher BE of 0.5 ± 0.1 and

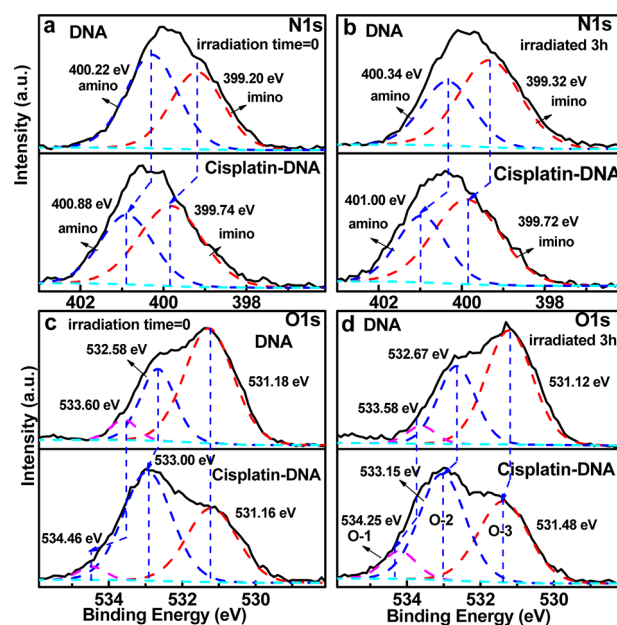


Figure 3. High-resolution XPS spectra comparison between DNA and cisplatin–DNA ($R = 8$) for N 1s (a, b), O 1s (c, d) both before and after irradiation for 3 h. The peaks of N 1s and O 1s spectra were deconvoluted to a few Gaussian components corresponding to respective species. Experimental data correspond to the solid curves and the Gaussian fits are shown by the dashed lines.

0.7 ± 0.1 eV, respectively, compared to that of DNA. Figure 3c illustrates that C–OH (O-1) and carbonyl group (O-2) show positive BE shifts of 0.4 ± 0.1 and 0.9 ± 0.1 eV with the

addition of cisplatin, while the O-3 exhibits no substantial BE shift.

After 3 h of continuous X-ray irradiation, all of three the O species in cisplatin–DNA complex show substantial positive BE shifts of 0.4 ± 0.1 , 0.5 ± 0.1 , and 0.7 ± 0.1 eV versus to that of DNA after identical processing (Figure 3d). Similarly, the BE of amino and imino species are also observed to shift by 0.4 ± 0.1 and 0.8 ± 0.1 eV after irradiation compared to that of irradiated DNA (Figure 3b).

The higher BE shifts of nitrogen and oxygen species for cisplatin–DNA complexes before irradiation corroborate the synergistic interaction between cisplatin and DNA, that is, the formation of chemical bond between Pt and N7 of G/A. Furthermore, the synergetic higher energy shifts after X-ray irradiation as the characterization of cisplatin-involved chemical reaction in chemotherapy are also observed by XPS. The more reducing percentage of 5.1 and 5.3% for O-3 (O–P–O) and O-2 (C=O) in the cisplatin–DNA complex in comparison with those of pure DNA, indicate that the O–P–O and C=O group tends to be the sensitive weak bonds in DNA with concomitant presence of cisplatin and X-ray irradiation. The decreasing of amino and imino in cisplatin–DNA complex are also more observed than those of in pure DNA after X-ray irradiation, that is, 30.2% versus 21.8% and 10% versus 4.7%, respectively. Overall, the results suggest the occurrence of a concomitant chemoradiation effect via the binding of cisplatin, which leads to the increase in sensitivity of DNA to X-rays.

The chemical bonds associated with the core elements having the most significant variation induced by this concomitant chemoradiation process can be identified from Table 1 as C-3 (C–N/C–O–C), O-3 (phosphate), amino (N–C), and phosphate. Specifically, the effective rate constants of C-3, O-3, and amino of cisplatin–DNA are 3.0-, 1.8-, and 1.9-folds larger than that of DNA. The enhancement values correlate well with the assigned bonds. The 3-folds increase damage of C-3 compared to 1.9-folds of the amino may be explained from the fact that C-3 reflects two types of C species, including C–N, which is amino from the perspective of N and C–O–C. Furthermore, the 1.8-folds increase rate constant of O-3 indicates breaking of backbone, most probably leading to the desorption of O-related species, but not P. The explanation of the similar rate constants of phosphate for DNA and cisplatin–DNA are not clear. One reason could be that the heavier P species are more difficult to desorb from the surface compared to O. The experiment of ESD for DNA biomolecules also shows that O related species, such as O^- and OH^- , could be detected, while no P species were observed.³⁷ Another explanation may be the relatively low XPS detection efficiency of the P signal compared to those of C, O, and N, which could result in the large deviation of P rate constants (Table 1). Nevertheless, the comparison of these rate constants shows that the cisplatin-induced radiosensitization preferentially increases the scissions of phosphodiester and N-glycosidic bonds in DNA.

It should be noted that the XPS spectra of C, N, O, and P elements for thymus DNA were similar to those of plasmid DNA. The same observation was made after binding with cisplatin at identical mole ratio of 1:8. This is not surprising since both types of DNA are biologically similar and generally constitute a representative target of double-strand DNA. The observation of no the XPS spectral shifts shows that the different amount of uncoiling of DNA caused by addition of Pt-agents and the different initial conformations result in the same

enhancement effect in bond breaking. Our results indicate that the role of cisplatin is essentially independent of the type of DNA target.

3.3. Secondary Electron Distribution of DNA and Cisplatin–DNA Complex. The SE distribution of DNA, cisplatin and cisplatin–DNA complexes were probed by recording the kinetic energy of emitted electrons induced by 1.5 keV X-ray irradiation. As shown in Figure 4, the integrated

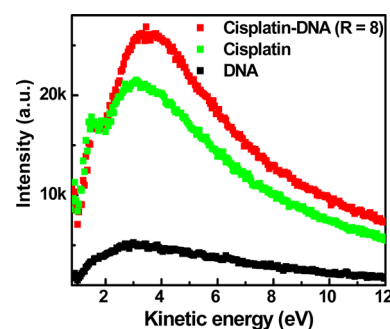


Figure 4. Secondary electrons distribution of DNA, cisplatin, and cisplatin–DNA with *R* of 8 induced by 1.5 keV X-ray.

number of SE produced from cisplatin–DNA complexes (*R* = 8) and cisplatin are significantly higher than that of pristine DNA, which provide the first experimental evidence of increase of production of LEE due to the presence of cisplatin. The dramatic difference indicates that the existence of cisplatin bound to DNA strongly promotes additional emission of SE during ionizing radiation. SE are known to be produced in large amounts by high-energy ionizing radiation. Most of them have kinetic energies below 20 eV.³⁸ When close to DNA these LEE can further cause single-strands, double-strand breaks, and other potentially lethal lesions, leading to mutagenic, genotoxic damages in cell.^{38–41} Kopyra et al. reported that cisplatin shows pronounced low-energy resonances feature at energies close to 0 eV.⁴² The resulting $[Pt(NH_2)_2]^-$ anion could decay by dissociative electron attachment creating reactive intermediate that would attack DNA. Our result provides further evidence that LEE are implicated in the mechanism of radiosensitization of DNA in concomitant chemoradiation therapy with Pt-based agents, as shown by the study of Zheng et al.¹⁴ Thus, the increase in damage not only arise from the sensitization of DNA to the action of secondary LEE, but also from an increase production of LEE at the site of binding of the cisplatin.

3.4. Role of Cisplatin on the Radiosensitization of DNA. Figure 5 presents the high-resolution Pt 4f spectra for cisplatin and cisplatin–thymus DNA complex with various exposures to X-ray irradiation. In order to obtain sufficient signal from Pt 4f spectra by XPS, in Figure 5 we increased the ratio of cisplatin to thymus DNA to 1 per 30 base pairs (bps) instead of the regular cisplatin–DNA mole ratio (*R* = 8) of 1:400 bps. Figure 5a,b exhibits the Pt 4f spectra of cisplatin with cisplatin–DNA complex at 0 and 130 min radiation. The chemical binding of Pt with DNA rises the Pt 4f peaks by about +1 eV compared to that of pure cisplatin. During the 130 min irradiation, the BEs of mainly two peaks, Pt 4f 5/2, 7/2, remains the same (Figure 5c). Surprisingly, a prominent shoulder peak initially contained in the spectrum of cisplatin–thymus gradually disappears with the continuous X-ray irradiation. At 130 min only the two peaks are clearly displayed (Figure 5c,e).

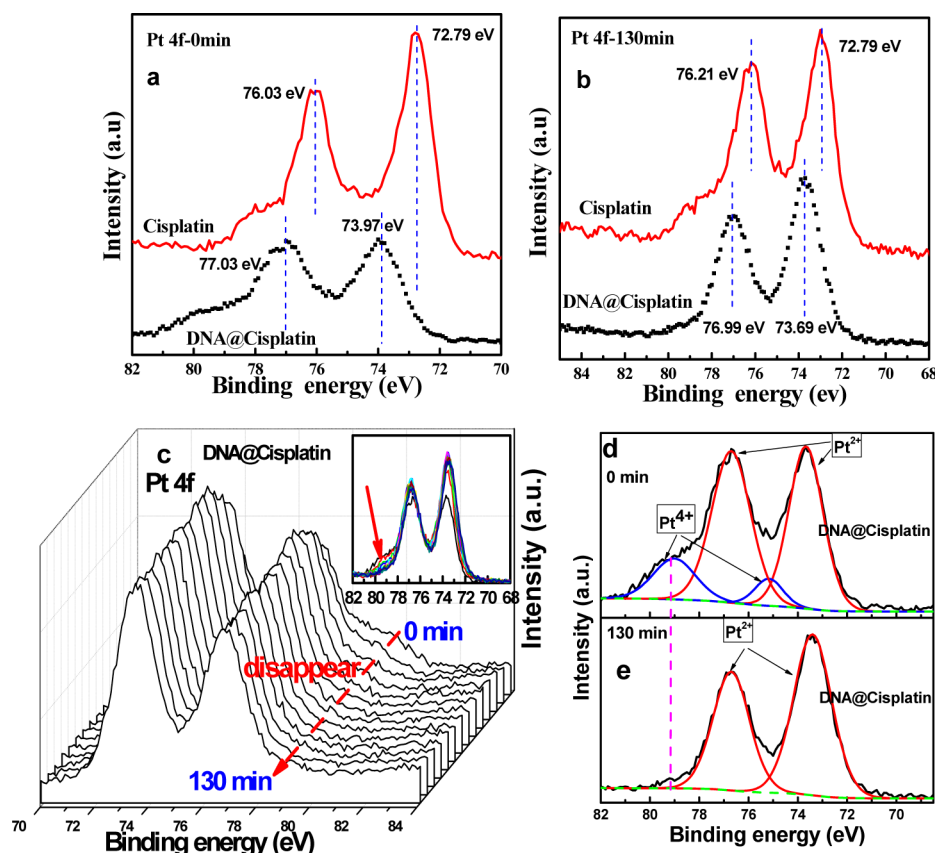


Figure 5. High-resolution Pt 4f spectra of cisplatin and cisplatin-thymus DNA at (a) initial irradiation time (0 min) and (b) continuously irradiated for 130 min. (c) The high-resolution Pt 4f spectra of cisplatin–thymus DNA obtained at interval of 10 min in the presence of soft X-ray irradiation. (d) The high-resolution Pt 4f spectra of cisplatin–thymus DNA at initial time (0 min) and (e) after 130 min irradiation.

The initial Pt 4f spectra of cisplatin–thymus could be deconvoluted into two pair of subpeaks (Figure 5d). The peaks with higher BE of 79.0 and 75.1 eV correspond to oxidation state Pt^{4+} . The assignment is based on the XPS spectrum of sodium hexachloroplatinate hexahydrate having a Pt^{4+} state located at higher BE compared to Pt^{2+} state.⁴³ While cisplatin is definitely a Pt^{2+} compound, it is reasonable to speculate that the formation of Pt^{4+} eludes from the oxidation of Pt^{2+} , that is, $\text{Pt}^{2+} \rightarrow \text{Pt}^{4+} + 2\text{e}^-$. With the irradiation of 1.5 keV X-ray, the oxidation reaction is energetic favored. On the other hand, the yield of another product of the reaction, electrons (2e^-) are consistent with the observation of the dramatic production of LEE from cisplatin and cisplatin–DNA complexes by X-ray. In other word, the increase of LEE for Pt-agents by high-energy radiation could be explained by the occurrence of the oxidation Pt^{2+} to Pt^{4+} . This reaction is particularly significant for the cisplatin–DNA complex since the formation of larger amount of LEE could easily interact with and transfer to the closely bound DNA molecules, leading to the increase cleavages of chemical bonds, particularly those of glycosidic and phosphodiester bonds. The oxidative Pt^{4+} is not stable and could easily convert back to Pt^{2+} . Thus, as the irradiation dose increases the existence of Pt^{4+} progressively disappears, leaving only two intrinsic peaks remaining in the Pt 4f spectra (Figure 5e).

CONCLUSION

The chemical bond transformation of cisplatin–DNA complexes can be probed efficiently by XPS, which provides a concomitant X-ray irradiation source as well. Substantial BE

shifts in terms of nitrogen and oxygen species in DNA and cisplatin–DNA complexes before and after irradiation, have revealed intense synergistic interaction between cisplatin and DNA under X-ray irradiation. The C–N/C–O–C (C-3), phosphate (O-3), and amino (N) are evidenced to be the most vulnerable bond scission sites in cisplatin–DNA complex. The ensemble of results demonstrates that typical chemoradiation process with involvement of cisplatin could greatly increase damage to DNA, specifically enhance the glycosidic and phosphodiester bond cleavages, which can be characterized as LEE-induced DNA damages. Compared to that of DNA, the rate constants of the above two bond scissions within cisplatin–DNA complexes are 1.9- and 1.8-folds larger. The formation of Pt^{4+} supports the occurrence of an oxidation reaction induced by X-rays, which is consistent with the increased production of LEE. Our results suggest that the presence of Pt could considerably increase formation of the SE in the direct effect of ionizing radiation and the further interaction of these LEE with DNA lead to the enhancement of bond cleavages. Although the condition in the cellular media with the adjacent of water molecules would be different, the understanding of the mechanism of cisplatin radiosensitization in the molecular level could have important implications in the improvement of cancer concomitant CRT particularly for the Pt-related drugs.

AUTHOR INFORMATION

Corresponding Author

*E-mail: yizheng@fzu.edu.cn.

Notes

The authors declare no competing financial interest.

■ ACKNOWLEDGMENTS

The support by the National Natural Science Foundation of China (20973039), the Award Program for Minjiang Scholar Professorship, Program for Changjiang Scholarship and Innovative Research Team in University (PCSIRT0818), National Basic Research Program of China (973 Program: 2007CB613306) is gratefully acknowledged. Thanks are also extended to Dr. Yunhui He for the assistance in XPS measurements.

■ REFERENCES

- (1) Rosenberg, B.; Vancamp, L.; Krigas, T. Inhibition of cell division in *Escherichia coli* by electrolysis products from a platinum electrode. *Nature* **1965**, *205*, 698–699.
- (2) Rosenberg, B.; Renshaw, E.; Vancamp, L.; Hartwick, J.; Drobnik, J. Platinum-induced filamentous growth in *Escherichia coli*. *J. Bacteriol.* **1967**, *93*, 716–721.
- (3) Rosenberg, B.; Camp, L.; Grimley, E.; Thomson, A. The inhibition of growth or cell division in *Escherichia coli* by different ionic species of platinum(IV) complexes. *J. Biol. Chem.* **1967**, *242*, 1347–1352.
- (4) Kelland, L. The resurgence of platinum-based cancer chemotherapy. *Nat. Rev. Cancer* **2007**, *7*, 573–584.
- (5) Jung, Y.; Lippard, S. J. Direct cellular responses to platinum-induced DNA damage. *Chem. Rev.* **2007**, *107*, 1387–1407.
- (6) Wong, E.; Giandomenico, C. M. Current status of platinum-based antitumor drugs. *Chem. Rev.* **1999**, *99*, 2451–2466.
- (7) Wang, D.; Lippard, S. J. Cellular processing of platinum anticancer drugs. *Nat. Rev. Drug Discovery* **2005**, *4*, 307–320.
- (8) Chu, G. Cellular responses to cisplatin. The roles of DNA-binding proteins and DNA repair. *J. Biol. Chem.* **1994**, *269*, 787–90.
- (9) Eastman, A. The formation, isolation and characterization of DNA adducts produced by anticancer platinum complexes. *Pharm. Ther.* **1987**, *34*, 155–166.
- (10) Sharma, V. M.; Wilson, W. R. Radiosensitization of advanced squamous cell carcinoma of the head and neck with cisplatin during concomitant radiation therapy. *Eur. Arch. Otorhinolaryngol.* **1999**, *256*, 462–465.
- (11) Kelland, L. R.; Farrell, N. *Platinum-Based Drugs in Cancer Therapy*; Humana Press Inc.: Totowa, NJ, 2000.
- (12) Devita, V. T.; et al. *Cancer: Principles and Practice of Oncology*; Williams and Wilkins: New York, 2011.
- (13) Kobayashi, K.; Frohlich, H.; Usami, N.; Takakura, K.; Le Sech, C. Enhancement of X-ray-induced breaks in DNA bound to molecules containing platinum: A possible application to hadrontherapy. *Radiat. Res.* **2002**, *157*, 32–37.
- (14) Zheng, Y.; Hunting, D. J.; Ayotte, P.; Sanche, L. Role of secondary low-energy electrons in the concomitant chemoradiation therapy of cancer. *Phys. Rev. Lett.* **2008**, *100*, 198101–1–4.
- (15) Sanche, L. Role of secondary low energy electrons in radiobiology and chemoradiation therapy of cancer. *Chem. Phys. Lett.* **2009**, *474*, 1–6.
- (16) Luo, T.; Yu, J.; Nguyen, J.; Wang, C.; Bristow, R. G.; Jaffray, D. A.; Zhou, X.; Lu, K.; Lu, Q.-B. Electron transfer-based combination therapy of cisplatin with tetramethyl-*p*-phenylenediamine for ovarian, cervical, and lung cancers. *Proc. Natl. Acad. Sci. U.S.A.* **2012**, *109*, 10175–10180.
- (17) Murakami, M.; Hirokawa, H.; Hayata, I. Analysis of radiation damage of DNA by atomic force microscopy in comparison with agarose gel electrophoresis studies. *J. Biochem. Biophys. Methods* **2000**, *44*, 31–40.
- (18) Theodorakis, C. W.; D'Surney, S. J.; Shugart, L. R. Detection of genotoxic insult as DNA strand breaks in fish blood cells by agarose gel electrophoresis. *Environ. Toxicol. Chem.* **1994**, *13*, 1023–1031.
- (19) Reeder, F.; Guo, Z.; Murdoch, P.; Corazza, A.; Hambley, T. W.; Berners-Price, S. J.; Chottard, J.; Sadler, P. J. Platination of A GG site on single-stranded and double-stranded forms of a 14-base oligonucleotide with diaqua cisplatin followed by NMR and HPLC. *Eur. J. Biochem.* **1997**, *249*, 370–382.
- (20) Volkova, E.; Dudones, L. P.; Bose, R. N. HPLC determination of binding of cisplatin to DNA in the presence of biological thiols: Implications of dominant platinum-thiol binding to its anticancer action. *Pharm. Res.* **2002**, *19*, 124–131.
- (21) Da Col, R.; Silvestro, L.; Baiocchi, C.; Giacosa, D.; Viano, I. High-performance liquid chromatographic–mass spectrometric analysis of *cis*-dichlorodiamineplatinum–DNA complexes using an ionspray interface. *J. Chromatogr.* **1993**, *633*, 119–128.
- (22) Warnke, U.; Rappel, C.; Meier, H.; Kloft, C.; Galanski, M.; Hartinger, C. G.; Keppler, B. K.; Jaehde, U. Analysis of platinum adducts with DNA nucleotides and nucleosides by capillary electrophoresis coupled to ESI-MS: Indications of guanosine 5'-monophosphate O6–N7 chelation. *Chem. Biol. Chem.* **2004**, *5*, 1543–1549.
- (23) Will, J.; Kys, A.; Sheldrick, W. S.; Wolters, D. Identification of (η 6-arene)ruthenium(II) protein binding sites in *E. coli* cells by combined multidimensional liquid chromatography and ESI tandem mass spectrometry: specific binding of [(η 6-*p*-cymene)-RuCl₂(DMSO)] to stress-regulated proteins and to helicases. *J. Biol. Inorg. Chem.* **2007**, *12*, 883–894.
- (24) Huels, M. A.; Boudaiffa, B.; Cloutier, P.; Hunting, D.; Sanche, L. Single, double, and multiple double strand breaks induced in DNA by 3–100 eV electrons. *J. Am. Chem. Soc.* **2003**, *125*, 4467–4477.
- (25) Cho, E.; Brown, A.; Kuech, T. F. Chemical Characterization of DNA-immobilized InAs surfaces using X-ray photoelectron spectroscopy and near-edge X-ray absorption fine structure. *Langmuir* **2012**, *28*, 11890–11898.
- (26) Ptasińska, S.; Stypczyńska, A.; Nixon, T.; Mason, N. J.; Klyachko, D. V.; Sanche, L. X-ray induced damage in DNA monitored by X-ray photoelectron spectroscopy. *J. Chem. Phys.* **2008**, *129*, 065102–1–6.
- (27) Ausubel, F.; Brent, R.; Kingston, R.; Moore, D.; Seidman, J.; Smith, J.; Struhl, K. *Current Protocols in Molecular Biology*; John Wiley & Sons Inc.: New York, 2003.
- (28) Manchester, K. L. Use of UV methods for measurement of protein and nucleic acid concentrations. *Biotechniques* **1996**, *20*, 968–970.
- (29) Manchester, K. L. Value of A260/A280 ratios for measurement of purity of nucleic acids. *Biotechniques* **1995**, *19*, 208–210.
- (30) Xiao, F.; Yao, X.; Bao, Q.; Li, D.; Zheng, Y. Sensitive marker of the cisplatin-DNA interaction: X-Ray photoelectron spectroscopy of CL. *Bioinorg. Chem. Appl.* **2012**, 649640.
- (31) Mirsaleh-Kohan, N.; Bass, A.; Sanche, L. Effect of morphology of thin DNA films on the electron stimulated desorption of anions. *J. Chem. Phys.* **2011**, *134*, 015102.
- (32) Abdoul-Carime, H.; Sanche, L. Sequence-specific damage induced by the impact of 3–30 eV electrons on oligonucleotides. *Radiat. Res.* **2001**, *156*, 151–157.
- (33) Von Sonntag, C. *Free-Radical-Induced DNA Damage and Its Repair*; Springer-Verlag: Berlin, Heidelberg, 2006.
- (34) Zheng, Y.; Cloutier, P.; Hunting, D. J.; Sanche, L.; Wagner, J. R. Chemical basis of DNA sugar–phosphate cleavage by low-energy electrons. *J. Am. Chem. Soc.* **2005**, *127*, 16592–16598.
- (35) Fichtinger-Schepman, A.; van Oosterom, A.; Lohman, P. Diamminedichloroplatinum(II)-induced DNA adducts in peripheral leukocytes from seven cancer patients: Quantitative immunochemical detection of the adduct induction and removal after a single dose of *cis*-diamminedichloroplatinum(II). *Cancer Res.* **1987**, *47*, 3000–3004.
- (36) Takahara, P.; Frederick, C.; Lippard, S. Crystal structure of the anticancer drug cisplatin bound to duplex DNA. *J. Am. Chem. Soc.* **1996**, *118*, 12309–12321.
- (37) Ptasińska, S.; Sanche, L. On the mechanism of anion desorption from DNA induced by low energy electrons. *J. Chem. Phys.* **2006**, *125*, 144713.

- (38) Lett, J. T.; Adler, H. I. *Advances in Radiation Biology*; Academic Press: New York, 1978.
- (39) Martin, F.; Burrow, P. D.; Cai, Z.; Cloutier, P.; Hunting, D.; Sanche, L. DNA strand breaks induced by 0–4 eV electrons: The role of shape resonances. *Phys. Rev. Lett.* **2004**, *93*, 068101–1–4.
- (40) LaVerne, J. A.; Pimblott, S. M. Electron energy-loss distributions in solid, dry DNA. *Radiat. Res.* **1995**, *141*, 208–215.
- (41) Cobut, V.; Frongillo, Y.; Pataut, J. P.; Goulet, T.; Fraser, M.-J.; Jay-Gerin, J. P. Monte Carlo simulation of fast electron and proton tracks in liquid water-I. Physical and physicochemical aspects. *Radiat. Phys. Chem.* **1998**, *51*, 229–243.
- (42) Kopyra, J.; Koenig-Lehmann, C.; Bald, I.; Illenberger, E. A single slow electron triggers the loss of both chlorine atoms from the anticancer drug cisplatin: Implications for chemoradiation therapy. *Angew. Chem.* **2009**, *48*, 7904–7907.
- (43) Guven, A.; Rusakova, I.; Lewis, M.; Wilson, L. Cisplatin@US-tube carbon nanocapsules for enhanced chemotherapeutic delivery. *Biomaterials* **2012**, *33*, 1455–1461.